

Home Page

Title Page

Contents



Page 1 of 20

Go Back

Full Screen

Close

Quit

## COMPUTATIONAL STUDY OF THE WILLMORE FLOW ON GRAPHS

TOMÁŠ OBERHUBER\*

**Abstract.** In this article we present two numerical schemes for the Willmore flow of graphs. Both of them are based on the method of lines. Resulting ordinary differential equations are solved using the 4th order Runge-Kutta-Merson solver. We show their numerical behaviour on several qualitative results and by computing experimental order of convergence.

**Key words.** Willmore flow, method of lines, curvature minimization, gradient flow, Laplace-Beltrami operator, Gauss curvature

**AMS subject classifications.** 35K35, 35K55, 53C44, 65M12, 65M20, 74S20

**1. Introduction.** In this article we consider evolution of two dimensional surface  $\Gamma(t)$  embedded in  $\mathbb{R}^3$  such that it can be described as a graph of some function  $u : (0, T) \times \Omega \rightarrow \mathbb{R}$ ,  $\Omega \subset \mathbb{R}^2$ . We computationally investigate the following law

$$V = 2\Delta_{\Gamma}H + H^3 - 4HK \text{ on } \Gamma(t), \quad (1.1)$$

where  $V$  is the normal velocity,  $\Delta_{\Gamma}$  is the Laplace-Beltrami operator,  $H = \kappa_1 + \kappa_2$  is the mean curvature,  $K = \kappa_1 \cdot \kappa_2$  is the Gauss curvature and  $\kappa_1$  and  $\kappa_2$  denote the principal curvatures of the surface.

As follows from [4, 5, 6] the law (1.1) represents the  $L_2$ -gradient flow for the functional

---

\*Faculty of Nuclear Sciences and Physical Engineering, Czech Technical University in Prague, Czech Republic [oberhuber@kmlinux.fjfi.cvut.cz](mailto:oberhuber@kmlinux.fjfi.cvut.cz)



$W$  defined as:

$$W(f) = \int_{\Gamma} H^2 \, dS, \quad \Gamma = \{(x, u(x)) \mid x \in \Omega\}. \quad (1.2)$$

The gradient flow approach is described e.g. in [11]. Existence of the solution under certain initial conditions was proved in [10, 7]. In [4] an implicit numerical scheme for the Willmore flow of graphs based on the finite element method together with the numerical analysis is presented. A level set formulation for the Willmore flow can be found in [5]. For the physical meaning of the minimization of (1.2) we refer to [3]. In [6] the authors describe an algorithm for evolution of elastic curves in  $\mathbb{R}^n$ . An interesting algorithm for parametrised curves driven by intrinsic Laplacian of curvature can be found in [8] where the authors use the tangential vector for redistribution of the control points on the curve. Application for the surface reconstruction of scratched objects is discussed in [12].

In this contribution, we explore the results presented in [9] and show computational behaviour of two finite-difference schemes incorporated into the method of lines. For discretization in time we use the 4th order Runge-Kutta type solver having explicit nature. This method was successfully used for solving several problems of the interface motion [1]. Our work is also related to [2] where the surface diffusion for graphs is treated by a similar approach.

**2. Problem formulation.** We assume that  $\Gamma(t)$  is a graph of a function  $u$  of two variables:

$$\Gamma(t) = \{[x, u(t, x)] \mid x \in \Omega \subset \mathbb{R}^2\},$$

where  $\Omega \equiv (0, L_1) \times (0, L_2)$  is an open rectangle,  $\partial\Omega$  its boundary and  $\nu$  its outer normal.

We express the quantities of (1.1) in terms of the graph description of  $\Gamma(t)$  – see [2]:

$$Q = \sqrt{1 + |\nabla u|^2}, \quad \mathbf{n} = \left(-1, \frac{\nabla u}{Q}\right), \quad V = -\frac{u_t}{Q},$$

$$H = \nabla \cdot \mathbf{n}, \quad K = \frac{\det D^2 u}{Q^4},$$

$$\Delta_\Gamma H = \frac{1}{Q} \nabla \cdot \left[ \left( QI - \frac{\nabla u \otimes \nabla u}{Q} \right) \nabla H \right].$$

LEMMA 2.1. For the graph formulation of the Willmore flow, (1.1) takes the following form

$$\frac{\partial u}{\partial t} = -Q \nabla \cdot \left[ \frac{2}{Q} (\mathbb{I} - \mathbb{P}) \nabla w - \frac{w^2}{Q^3} \nabla u \right], \quad (2.1)$$

$$w = Q \nabla \cdot \frac{\nabla u}{Q}, \quad (2.2)$$

where

$$\mathbb{P} = \frac{\nabla u}{Q} \otimes \frac{\nabla u}{Q}, \quad (u \otimes v)_{ij} = u_i \cdot v_j.$$

The proof of this lemma can be found in [4] or [9]. It allows to introduce the following problem:

DEFINITION 2.2. The graph formulation for the Willmore flow is a system of two partial

differential equations of the second order for  $u$  and  $w$

$$\frac{\partial u}{\partial t} = -Q\nabla \cdot \left[ \frac{2}{Q} (\mathbb{I} - \mathbb{P}) \nabla w - \frac{w^2}{Q^3} \nabla u \right] \text{ in } \Omega \times (0, T), \quad (2.3)$$

$$w = Q\nabla \cdot \frac{\nabla u}{Q}, \quad (2.4)$$

$$u(\cdot, 0) = u_{ini},$$

with the Dirichlet boundary conditions

$$u|_{\partial\Omega} = 0, \quad w|_{\partial\Omega} = 0, \quad (2.5)$$

or with the Neumann boundary conditions

$$\frac{\partial u}{\partial \nu} |_{\partial\Omega} = 0, \quad \frac{\partial w}{\partial \nu} |_{\partial\Omega} = 0. \quad (2.6)$$

According to [9] we can define the weak solution for the Willmore flow of graphs as follows:

**DEFINITION 2.3.** The weak solution of the graph formulation for the Willmore flow with homogeneous Dirichlet boundary conditions is a couple  $u, w : (0, T) \rightarrow H_0^1(\Omega)$  which satisfy a.e in  $(0, T)$ , for each test functions  $\varphi, \xi \in H_0^1(\Omega)$

$$\int_{\Omega} \frac{u_t}{Q} \varphi = \int_{\Omega} \frac{2}{Q} (\mathbb{I} - \mathbb{P}) \nabla w \nabla \varphi - \int_{\Omega} \frac{w^2}{Q^3} \nabla u \nabla \varphi \text{ a.e. in } (0, T) \quad (2.7)$$

$$\int_{\Omega} \frac{w}{Q} \xi = - \int_{\Omega} \frac{\nabla u}{Q} \nabla \xi. \quad (2.8)$$

with the initial condition

$$u|_{t=0} = u_{ini}.$$



Weak solution for the problem with homogeneous Neumann boundary conditions is a couple  $u, w : (0, T) \rightarrow H^1(\Omega)$  which satisfy (2.7) a.e. in  $(0, T)$ , for each test functions  $\varphi, \xi \in H^1(\Omega)$ .

REMARK: There are at least two different steady solutions for the Willmore flow of graphs. The trivial solution is represented by a constant function  $u$  (specified by the boundary conditions) and zero mean curvature ( $w = 0$ ). The second solution is induced by a sphere with given radius  $r$  since the principal curvatures are  $\kappa_1 = \kappa_2 = \frac{1}{r}$  and so  $H = \kappa_1 + \kappa_2 = \frac{2}{r}$  and  $K = \kappa_1 \kappa_2 = \frac{1}{r^2}$ . From this fact it follows that the right hand side of (1.1) is equal to zero. In this case, the boundary conditions are different from (2.5) and (2.6).

Mathematical properties of (1.1) have been partially studied in [10] for the case when the initial condition is close to a sphere and in [7] existence of the solution was proved under the assumption that  $\int_{\Gamma} |A^\circ|^2$  is sufficiently small, for  $A^\circ$  denoting the trace-free part of the second fundamental form.

**3. Numerical schemes.** For the numerical solution of (1.1), we will use method of lines with the finite difference discretization in space. We will derive both, the scheme based on combination of backward and forward formulas, and the scheme based on central formulas.

We use the following notation. Let  $h_1, h_2$  be space steps such that  $h_1 = \frac{L_1}{N_1}$  and  $h_2 = \frac{L_2}{N_2}$  for some  $N_1, N_2 \in \mathbb{N}$ . We define a uniform grid as

$$\begin{aligned} \omega_h &= \{(ih_1, jh_2) \mid i = 1 \cdots N_1 - 1, j = 1 \cdots N_2 - 1\}, \\ \bar{\omega}_h &= \{(ih_1, jh_2) \mid i = 0 \cdots N_1, j = 0 \cdots N_2\}. \end{aligned}$$

For  $u : \mathbb{R}^2 \rightarrow \mathbb{R}$  we define a projection on  $\bar{\omega}_h$  as  $u_{ij} = u(ih_1, jh_2)$ . We introduce the

differences as follows

$$\begin{aligned} u_{\bar{x}_1,ij} &= \frac{u_{ij} - u_{i-1,j}}{h_1}, & u_{\bar{x}_2,ij} &= \frac{u_{ij} - u_{i,j-1}}{h_2}, \\ u_{x_1,ij} &= \frac{u_{i+1,j} - u_{ij}}{h_1}, & u_{x_2,ij} &= \frac{u_{i,j+1} - u_{ij}}{h_2}, \\ u_{\hat{x}_1,ij} &= \frac{u_{i+1,j} - u_{i-1,j}}{2h_1}, & u_{\hat{x}_2,ij} &= \frac{u_{i,j+1} - u_{i,j-1}}{2h_2}, \end{aligned}$$

$$\bar{\nabla}_h u_{ij} = (u_{\bar{x}_1,ij}, u_{\bar{x}_2,ij}), \quad \nabla_h u_{ij} = (u_{x_1,ij}, u_{x_2,ij}), \quad \hat{\nabla}_h u_{ij} = (u_{\hat{x}_1,ij}, u_{\hat{x}_2,ij}).$$

For the discretization of the Neumann boundary conditions we define the grid boundary normal difference  $u_{\bar{n}}$ :

$$\begin{aligned} u_{\bar{n},0j} &= u_{\bar{x}_1,1j} & \text{and} & & u_{\bar{n},N_1j} &= u_{\bar{x}_1,N_1j} & \text{for } j = 0, \dots, N_2, \\ u_{\bar{n},i0} &= u_{\bar{x}_2,i1} & \text{and} & & u_{\bar{n},iN_2} &= u_{\bar{x}_2,iN_2} & \text{for } i = 0, \dots, N_1. \end{aligned}$$

If we denote

$$\begin{aligned} \bar{Q}_{ij} &= \sqrt{1 + \frac{1}{2} \left( u_{\bar{x}_1,ij}^2 + u_{x_1,ij}^2 + u_{\bar{x}_2,ij}^2 + u_{x_2,ij}^2 \right)}, & i = 1, \dots, N_1 - 1, \quad j = 1, \dots, N_2 - 1, \\ Q_{ij} &= \sqrt{1 + u_{\bar{x}_1,ij}^2 + u_{\bar{x}_2,ij}^2}, & i = 1, \dots, N_1, \quad j = 1, \dots, N_2, \\ \mathbb{E}_{ij} &= \frac{2}{Q_{ij}} \begin{pmatrix} 1 - u_{\bar{x}_1,ij}^2 & -u_{\bar{x}_1,ij} u_{\bar{x}_2,ij} \\ -u_{\bar{x}_1,ij} u_{\bar{x}_2,ij} & 1 - u_{\bar{x}_2,ij}^2 \end{pmatrix}, & i = 1, \dots, N_1, \quad j = 1, \dots, N_2. \end{aligned}$$

then *the first scheme* has the following form

$$\frac{du^h}{dt} = -\bar{Q} \nabla_h \left( \frac{2}{Q} \mathbb{E} \bar{\nabla}_h w^h - \frac{(w^h)^2}{Q^3} \bar{\nabla}_h u^h \right), \quad (3.1)$$

$$w^h = Q \cdot \left[ \left( \frac{u^h_{\bar{x}_1}}{Q} \right)_{x_1} + \left( \frac{u^h_{\bar{x}_2}}{Q} \right)_{x_2} \right]. \quad (3.2)$$

For

$$\begin{aligned} \mathring{Q}_{ij} &= \sqrt{1 + u_{\mathring{x}_1, ij}^2 + u_{\mathring{x}_2, ij}^2}, & i = 1, \dots, N_1, \quad j = 1, \dots, N_2, \\ \mathring{\mathbb{E}}_{ij} &= \frac{2}{\mathring{Q}_{ij}} \begin{pmatrix} 1 - u_{\mathring{x}_1, ij}^2 & -u_{\mathring{x}_1, ij} u_{\mathring{x}_2, ij} \\ -u_{\mathring{x}_1, ij} u_{\mathring{x}_2, ij} & 1 - u_{\mathring{x}_2, ij}^2 \end{pmatrix}, & i = 1, \dots, N_1, \quad j = 1, \dots, N_2, \end{aligned}$$

the second scheme has the following form

$$\frac{du^h}{dt} = -\bar{Q} \mathring{\nabla}_h \left( \frac{2}{\mathring{Q}} \mathring{\mathbb{E}} \mathring{\nabla}_h w^h - \frac{(w^h)^2}{\mathring{Q}^3} \mathring{\nabla}_h u^h \right), \quad (3.3)$$

$$w^h = \mathring{Q} \cdot \left[ \left( \frac{u^h}{\mathring{Q}} \right)_{\mathring{x}_1} + \left( \frac{u^h}{\mathring{Q}} \right)_{\mathring{x}_2} \right]. \quad (3.4)$$

For both schemes we set the initial condition as

$$u^h(0) = u_{ini} |_{\bar{\omega}_h},$$

and we consider either the Dirichlet boundary conditions

$$u^h |_{\partial\omega_h} = 0, \quad w^h |_{\partial\omega_h} = 0, \quad (3.5)$$

or the Neumann boundary conditions

$$u_{\bar{n}}^h |_{\partial\omega_h} = 0, \quad w_{\bar{n}}^h |_{\partial\omega_h} = 0. \quad (3.6)$$

The following theorem shows the energy equality of the scheme (3.1)–(3.2).

**THEOREM 3.1.** *For  $u^h |_{\partial\omega_h} = 0$  and  $w^h = 0 |_{\partial\omega_h}$  the solution of (3.1)–(3.2) satisfies*

$$\frac{1}{2} \left( (u_t^h)^2, \frac{1}{Q} \right)_h + \frac{1}{2} \frac{d}{dt} \left( (w^h)^2, \frac{1}{Q} \right)_h = 0.$$

The proof of the theorem can be found in [9].

**4. Computational results.** In this section we analyse both schemes from the viewpoint of numerical convergence and of qualitative behaviour. Since any analytical solution for the Willmore flow is not known we solved the equation (2.3) with additional terms on the right hand side. We changed the equation in such way that it has analytical solution  $u_{test}(x, t) = \sin(\pi x) \cdot e^{-100t}$  – see FIG. 4.1

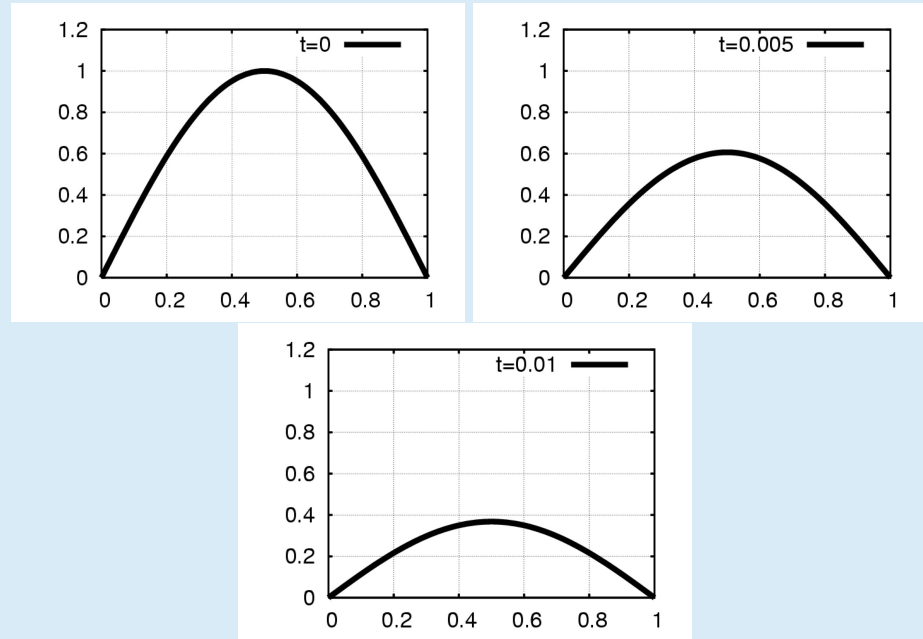


FIG. 4.1. Decay towards a planar surface at times  $t = 0$ ,  $t = 0.005$  and  $t = 0.01$ .

$N$	$h$	EOC $E_1$	EOC $E_\infty$	$E_1$	$E_\infty$
20	0.0526	6.9180	5.9651	0.00275	0.01344
30	0.0344	5.0545	4.0265	0.00032	0.00244
40	0.0256	1.6705	2.3854	0.00019	0.00120
50	0.0204	2.1441	2.3586	0.00012	0.00070
60	0.0169	2.3809	2.4314	7.80264e-05	0.00044
70	0.0144	2.5189	2.4497	5.25966e-05	0.00030
80	0.0126	2.6127	2.5947	3.69297e-05	0.00021
90	0.0112	2.6784	2.5884	2.68374e-05	0.00015
100	0.0101	2.7267	2.6773	2.00742e-05	0.00011

TABLE 4.1  
EOC for the forward-backward scheme (3.1)–(3.2)

The resulting equation takes the following form

$$\begin{aligned} \frac{\partial u}{\partial t} = & -Q\nabla \cdot \left[ \frac{2}{Q} (\mathbb{I} - \mathbb{P}) \nabla w - \frac{w^2}{Q^3} \nabla u \right] \\ & - \frac{\partial u_{test}}{\partial t} + Q_{test} \nabla \cdot \left[ \frac{2}{Q_{test}} (\mathbb{I} - \mathbb{P}_{test}) \nabla w_{test} - \frac{w_{test}^2}{Q_{test}^3} \nabla u_{test} \right], \end{aligned}$$

for

$$Q_{test} = \sqrt{1 + |\nabla u_{test}|^2}, \quad \mathbb{P}_{test} = \frac{\nabla u_{test}}{Q_{test}} \otimes \frac{\nabla u_{test}}{Q_{test}}, \quad w_{test} = Q_{test} \nabla \cdot \frac{\nabla u_{test}}{Q_{test}}.$$

Since we performed the computation on the interval  $(0, 1)$  we set the following time dependent Dirichlet boundary conditions

$$\begin{aligned} u^h|_{x=0} &= 0, & u^h|_{x=1} &= 0, \\ w^h|_{x=0} &= w_{test}|_{x=0}, & w^h|_{x=1} &= w_{test}|_{x=1}. \end{aligned}$$

$N$	$h$	EOC $E_1$	EOC $E_\infty$	$E_1$	$E_\infty$
20	0.0526	6.9180	5.9651	0.00275	0.01344
40	0.0256	3.6604	3.3504	0.00019	0.00120
80	0.0126	2.3794	2.4432	3.69297e-05	0.00021

TABLE 4.2

EOC for the forward-backward scheme (3.1)–(3.2) in case of doubling grid size

$N$	$h$	EOC $E_1$	EOC $E_\infty$	$E_1$	$E_\infty$
20	0.05263	4.9505	3.8605	0.01171	0.06239
30	0.03448	7.3301	6.8252	0.00052	0.00348
40	0.02564	4.6028	5.1642	0.00013	0.00075
50	0.02040	3.6558	2.8342	5.86225e-05	0.00039
60	0.01694	3.6106	3.0554	2.99810e-05	0.00022
70	0.01449	3.7137	3.2093	1.67618e-05	0.00013
80	0.01265	3.7593	3.3069	1.00772e-05	8.65410e-05
90	0.01123	3.7552	3.4530	6.44126e-06	5.73444e-05
100	0.01010	3.7184	3.5785	4.33514e-06	3.91735e-05
110	0.00917	3.8483	3.7392	2.99349e-06	2.73352e-05
120	0.00840	3.9727	3.3529	2.11220e-06	2.03661e-05
130	0.00775	3.4604	1.7160	1.59762e-06	1.77327e-05
140	0.00719	4.2264	4.8064	1.16527e-06	1.23858e-05
150	0.00671	3.3477	4.4887	9.23473e-07	9.06765e-06
160	0.00628	4.3818	4.4219	6.94718e-07	6.80376e-06

TABLE 4.3

EOC for the central scheme (3.3)–(3.4)

Home Page

Title Page

Contents



Page 11 of 20

Go Back

Full Screen

Close

Quit

$N$	$h$	EOC $E_1$	EOC $E_\infty$	$E_1$	$E_\infty$
20	0.05263	4.95058	3.86058	0.01171	0.06239
40	0.02564	6.20653	6.14099	0.00013	0.00075
80	0.01265	3.67665	3.06628	1.00772e-05	8.65410e-05
160	0.00628	3.82374	3.63589	6.94718e-07	6.80376e-06

TABLE 4.4

EOC for the central scheme (3.3)–(3.4) in case of doubling grid size

Home Page

Title Page

Contents



Page 12 of 20

Go Back

Full Screen

Close

Quit

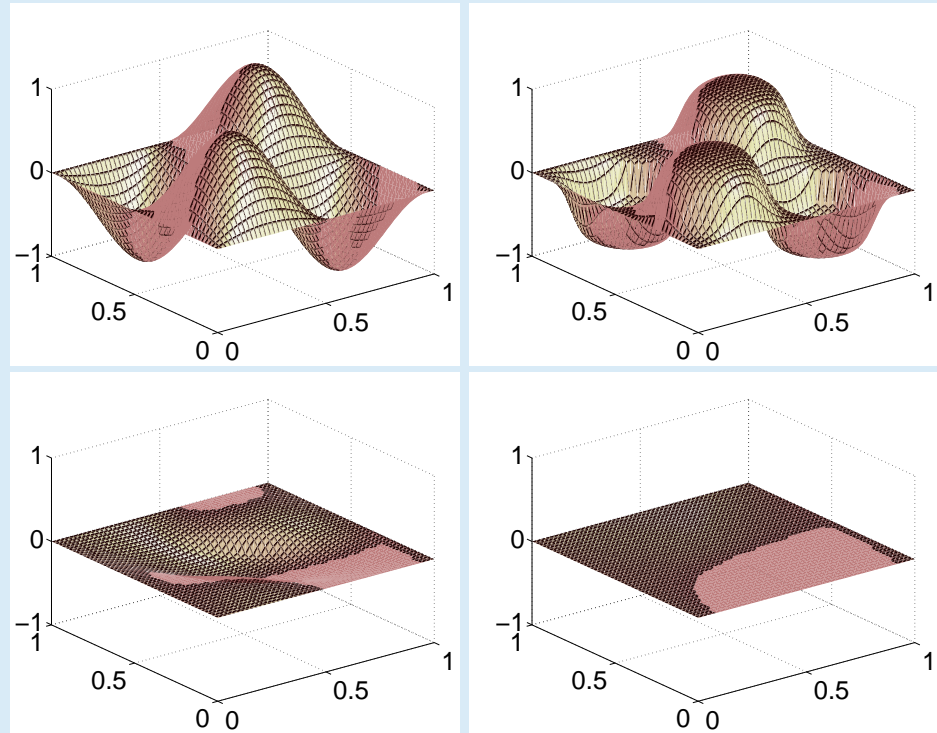


FIG. 4.2. Decay towards the planar surface at times  $t = 0$ ,  $t = 10^{-4}$ ,  $t = 17 \cdot 10^{-4}$  and  $t = 0.01$ .

Home Page

Title Page

Contents



Page 13 of 20

Go Back

Full Screen

Close

Quit

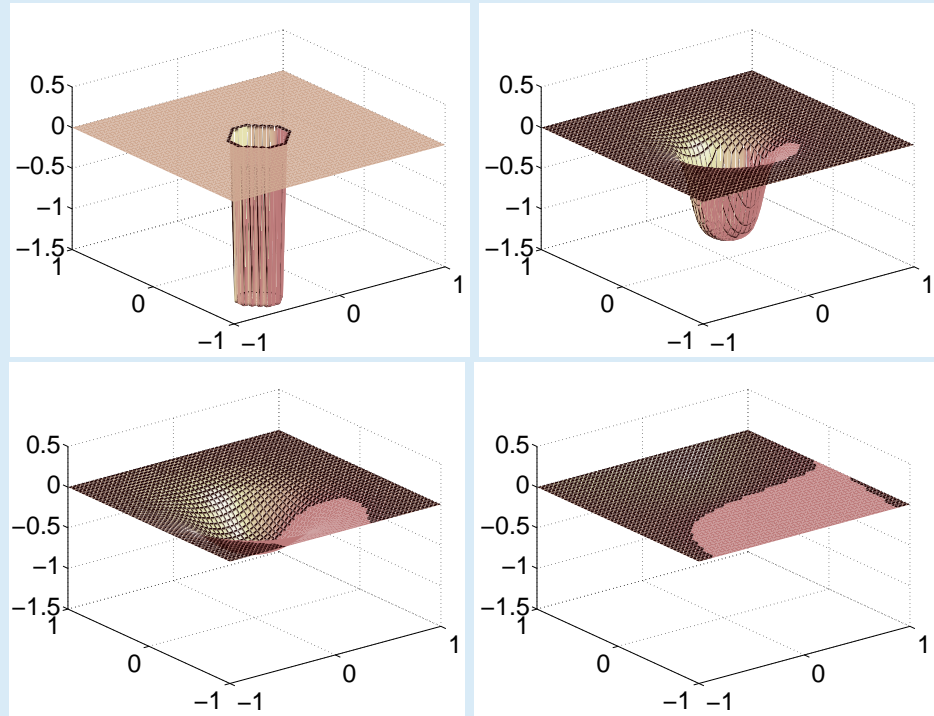


FIG. 4.3. Decay towards the planar surface at times  $t = 0$ ,  $t = 0.002$ ,  $t = 0.005$  and  $t = 1$ .

Home Page

Title Page

Contents



Page 14 of 20

Go Back

Full Screen

Close

Quit

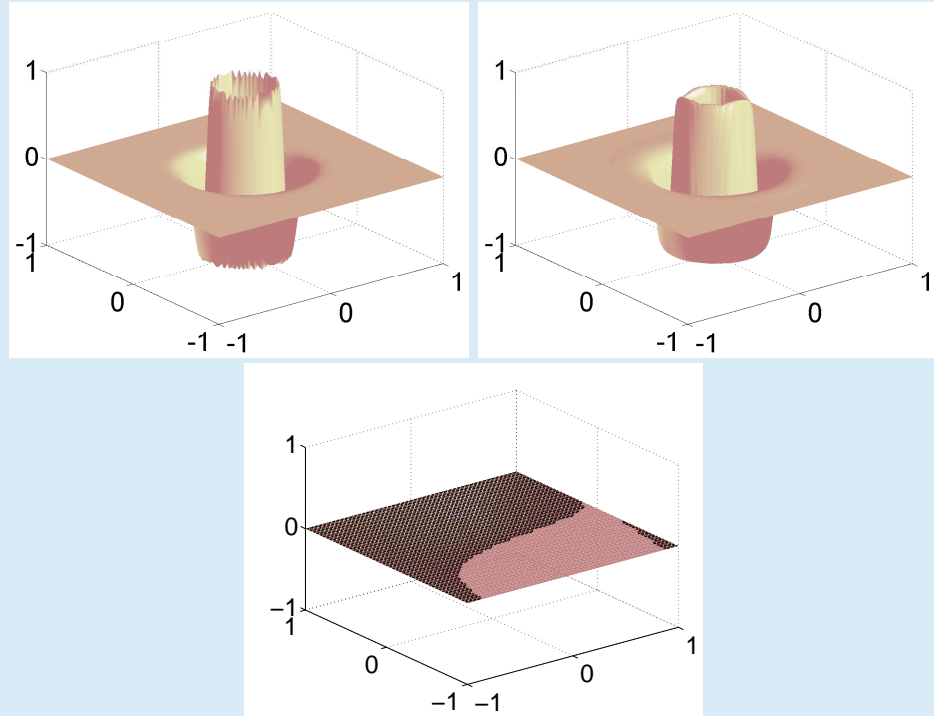


FIG. 4.4. Decay towards the planar surface at times  $t = 0$ ,  $t = 5 \cdot 10^{-6}$  and  $t = 0.1$ .

Home Page

Title Page

Contents



Page 15 of 20

Go Back

Full Screen

Close

Quit

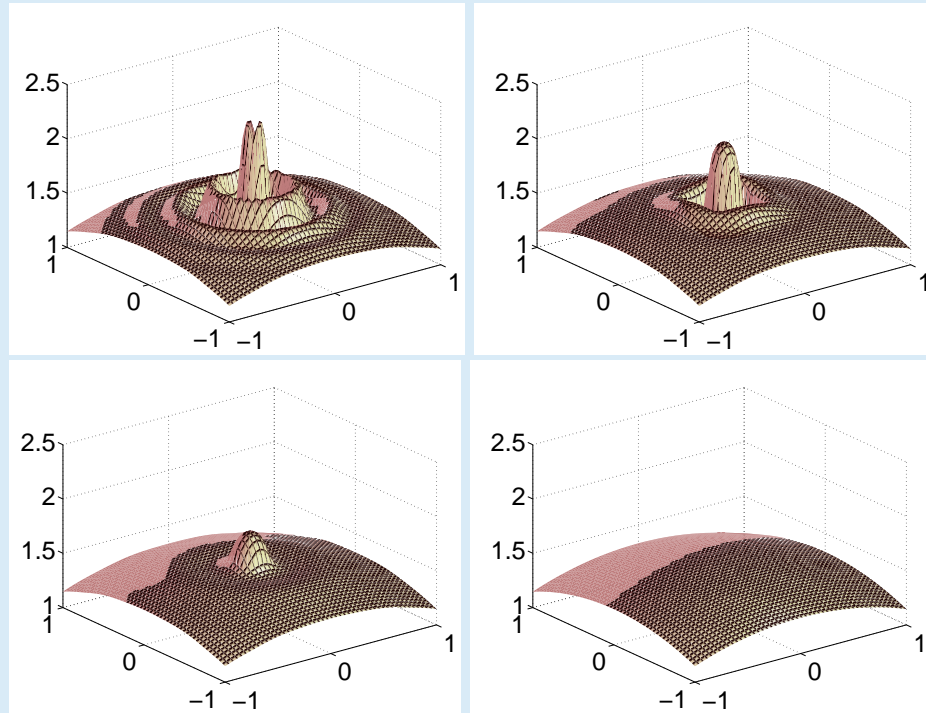


FIG. 4.5. Spherical surface restoration at times  $t = 0$ ,  $t = 2 \cdot 10^{-5}$ ,  $t = 10^{-4}$  and  $t = 0.05$ .

Home Page

Title Page

Contents



Page 16 of 20

Go Back

Full Screen

Close

Quit

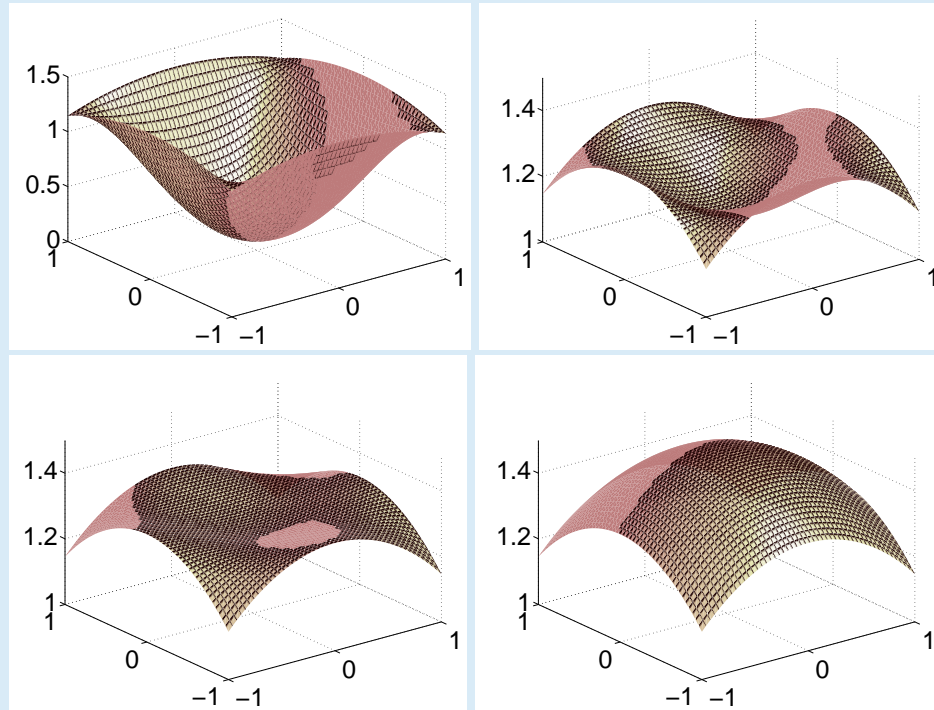


FIG. 4.6. Spherical surface restoration at times  $t = 0$ ,  $t = 0.05$ ,  $t = 0.06$  and  $t = 0.2$ .

Home Page

Title Page

Contents



Page 17 of 20

Go Back

Full Screen

Close

Quit

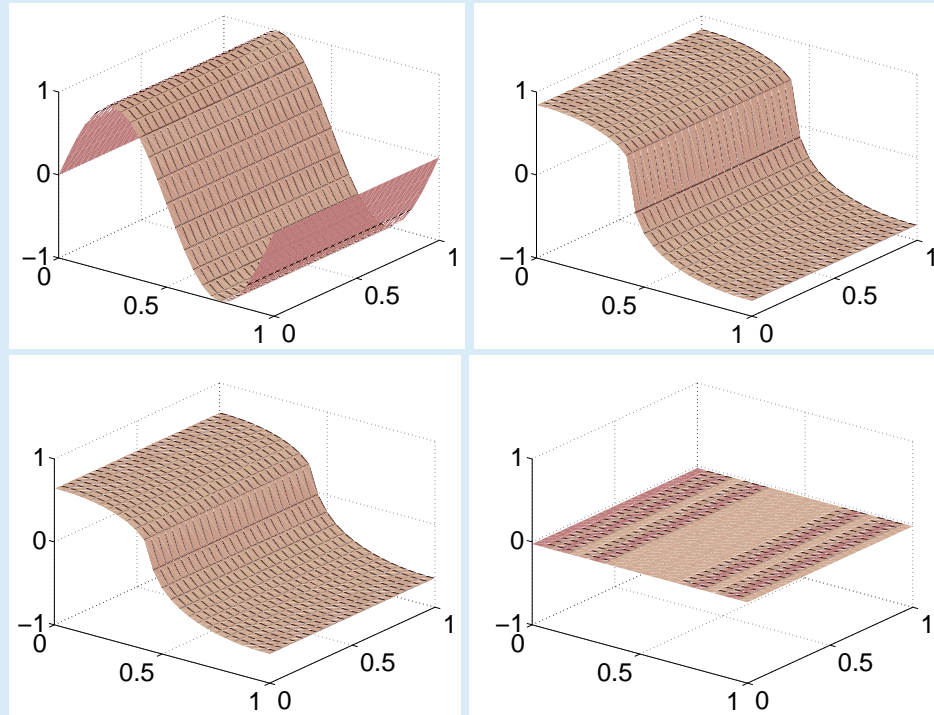


FIG. 4.7. Test with the Neumann boundary conditions at times  $t = 0$ ,  $t = 0.005$ ,  $t = 0.175$  and  $t = 0.5$ .

We evaluate the errors of computation on a grid with the space step  $h_i$  according to

$$E_\infty^{h_i} = \max_{j=0, \dots, N_i-1} |u_j^{h_i} - u_{test}(jh_i)|, \quad E_1^{h_i} = \sum_{j=0}^{N_i-1} |u_j^{h_i} - u_{test}(jh_i)|,$$

where  $N_i = 1/h_i$ . Then for two different space steps  $h_i, h_j$  we compute the experimental order of convergence as

$$\text{EOC } E_\infty^{h_i h_j} = \frac{\ln(E_\infty^{h_i}/E_\infty^{h_j})}{\ln(h_i/h_j)}, \quad \text{EOC } E_1^{h_i h_j} = \frac{\ln(E_1^{h_i}/E_1^{h_j})}{\ln(h_i/h_j)}. \quad (4.1)$$

The results for the forward-backward scheme (3.1)–(3.2) are concluded in TABLES 4.1 and 4.2. For the central scheme (3.3)–(3.4) see TABLES 4.3 and 4.4.

In the following we present several numerical experiments of qualitative character. First three examples show a decay towards a planar surface. For all of them we considered homogeneous Dirichlet boundary conditions for  $u$  and  $w$ . FIG. 4.2 shows evolution of the initial condition  $u_{ini}(x, y) = \sin(2\pi x) \cdot \sin(2\pi y)$  on the domain  $\Omega \equiv (0, 1)^2$  with  $50 \times 50$  meshes and the space steps  $h_1 = h_2 = 0.02$ . The computation has been performed until the time  $T = 0.01$ .

In the FIG. 4.3 we show again a decay towards a planar surface. The initial condition is discontinuous:  $u_{ini}(x, y) = \text{sign}(x^2 + y^2 - 0.2)$ . The domain  $\Omega$  is  $(-1, 1)^2$  and there are again  $50 \times 50$  meshes and  $h_1 = h_2 = 0.04$ . We stopped the computation at the time  $T = 1$ .

The FIG. 4.4 shows a decay towards the planar surface with highly oscillating initial condition  $u_{ini}(x, y) = \sin\left[2\pi\left(15 \tanh\left(\sqrt{x^2 + y^2} - 0.2\right)\right)\right]$ . The domain  $\Omega$  is  $(-1, 1)^2$  and there are  $50 \times 50$  meshes and  $h_1 = h_2 = 0.04$ . The final time for the computation was  $T = 0.1$ .

Next two examples show the restoration of a spherical surface. We start with a part of the sphere with radius  $R = 3$  and center  $C = (0, 0, -1.5)$  above the square domain  $\Omega \equiv (-1, 1)^2$ .

We obtain a graph which can be described by a function  $u_S$ . It yields  $w_S = Q(u_S)H(u_S)$ . Then the following Dirichlet boundary conditions

$$u|_{\partial\omega_h} = u_S, \quad w|_{\partial\omega_h} = w_S,$$

are considered (they are more general than (2.5) and (2.6)). In case of FIG. 4.5 we perturb the original function  $u_S$  as follows

$$u_{ini} = u_S + \exp^{-5r} \cdot \sin(7.5\pi r),$$

for  $r = \sqrt{x^2 + y^2}$ . The initial condition for FIG. 4.6 was obtained by applying the heat equation on the initial function  $v_{ini} \equiv 0$  with the Dirichlet boundary conditions  $v|_{\partial\omega_h} = u_S$  and setting  $u_{ini} = v|_{t=0.1}$ . There were  $50 \times 50$  meshes and  $h_1 = h_2 = 0.04$  in both cases. In the first case (FIG. 4.5) we stopped the computation at the time  $T = 0.05$  and in the second case (FIG. 4.6) at  $T = 0.2$ .

The example on FIG. 4.7 shows a computation with the homogeneous Neumann boundary conditions (3.6). The initial condition is  $u_0(x, y) = \sin(2\pi x)$  on  $\Omega = (0, 1)^2$  with  $25 \times 25$  meshes and  $h_1 = h_2 = 0.04$ . The final time  $T = 0.5$ .

**5. Conclusion.** In this article, we presented two numerical schemes for the Willmore flow of graphs. We computed experimental order of convergence for both of them together with several numerical experiments.

**6. Acknowledgement.** This work has been partially supported by Czech Technical University with grant No. CTU0508414 and by the Ministry of Education of the Czech Republic under the research plan No. MSM 6840770010.

## REFERENCES

- [1] M. Beneš, *Diffuse-Interface Treatment of the Anisotropic Mean-Curvature Flow*, Applications of Mathematics, **48**(6), (2003) 437–453.

[Home Page](#)

[Title Page](#)

[Contents](#)



Page 20 of 20

[Go Back](#)

[Full Screen](#)

[Close](#)

[Quit](#)

- [2] M. Beneš, *Numerical Solution for Surface Diffusion on Graphs*, submitted to the Proceedings on the Czech-Japanese Seminar in Applied Mathematics 2005.
- [3] P. Ciarlet, *Mathematical Elasticity, Vol III: Theory of Shells*, North-Holland, 2000.
- [4] K. Deckelnick and G. Dziuk, *Error estimates for the Willmore flow of graphs*.
- [5] M. Droske and M. Rumpf, *A level set formulation for Willmore flow*, *Interfaces and Free Boundaries*, **6**(3) (2004), 361–378.
- [6] G. Dziuk, E. Kuwert and R. Schatzle, *Evolution of Elastic Curves in  $\mathbb{R}^n$ : Existence and Computation*, *SIAM J. Math. Anal.* **41**(6), (2003), 2161–2179.
- [7] E. Kuwert and R. Schatzle, *The Willmore flow with small initial energy*, *Journal of Differential Geometry*, **57** (2001), 409–441.
- [8] K. Mikula and D. Ševčovič, *Tangentially Stabilized Lagrangian Algorithm for Elastic Curve Evolution Driven by Intrinsic Laplacian of Curvature*, *Proceedings of ALGORITMY 2005*, 1–10.
- [9] T. Oberhuber, *Numerical Solution of the Willmore flow on Graphs*, submitted to the Proceedings on the Czech-Japanese Seminar in Applied Mathematics 2005.
- [10] G. Simonett, *The Willmore flow near spheres*, *Differential and Integral Equations* **14**(8) (2001), 1005–1014.
- [11] J. E. Taylor and J. W. Cahn, *Linking Anisotropic Sharp and Diffuse Surface Motion Laws via Gradient Flows*, *J. Statist. Phys.*, **77** (1994), 183–197.
- [12] U. Clarenz, U. Diewald, G. Dziuk, M. Rumpf and R. Rusu, *A finite element method for surface restoration with smooth boundary conditions*, *Computer Aided Geometric Design* **21**(5) (2004), 427–445.